Int. J. Electrochem. Sci., 15 **(2020)** 6572 – 6581, doi: 10.20964/2020.07.50

International Journal of
ELECTROCHEMICAL
SCIENCE
www.electrochemsci.org

Stress Corrosion Cracking of 05Cr17Ni4Cu4Nb and 1Cr12Ni3Mo2VN Martensitic Stainless Steels under Constant Load

Wenming Tian[*], *Fangfang Chen, Zhonglei Li, Guoxing Pang, Yanxia Li*

School of Materials Engineering, North China Institute of Aerospace Engineering, No.133 Aimindong Road, Langfang Hebei Province 065000, China.
[*]E-mail: tianwenming.dhr@163.com

Received: 18 February 2020 / *Accepted:* 15 April 2020 / *Published:* 10 June 2020

The stress corrosion cracking (SCC) of martensitic stainless steel was evaluated in 5 wt.% NaCl solution under constant load with different stress levels. Results showed that the strength loss of 05Cr17Ni4Cu4Nb at the stress levels of 95%σ0.2, 90%σ0.2, 85%σ0.2 and 80%σ0.2 was 3.05%, 2.46%, 0.57% and 0.21% , respectively; the corresponding strength loss of 1Cr12Ni3Mo2VN at such stress levels was 3.76%, 3.09%, 1.42% and 0.49%, respectively. The stress corrosion resistance of 05Cr17Ni4Cu4Nb was better than that of the 1Cr12Ni3Mo2VN. The electrochemical measurements revealed that the passive potential range of 05Cr17Ni4Cu4Nb (from -0.15 to 0.12V) was wider than that of the 1Cr12Ni3Mo2VN (from -0.15 to -0.02V). A better passive film was formed on the surface of 05Cr17Ni4Cu4Nb, which led to a better stress corrosion resistance for 05Cr17Ni4Cu4Nb.

Keywords: A. Constant load; B. SCC; C. Martensitic stainless steels; D. Electrochemical measurement; E. Corrosion

1. INTRODUCTION

Martensitic stainless steel is a type of low carbon or high carbon steels containing 12 wt.% to 18 wt.% chromium element, and widely used in industries such as cutting tools, cutlery and high strength structural component because of its high mechanical properties and moderate corrosion resistance. While, in the most commonly industry environment, martensitic stainless steel usually encounters localized corrosion and stress corrosion cracking (SCC) due to the existence of aggressive ions such as chloride ion [1-10]. Stress corrosion cracking of martensitic stainless steel always results in huge damage of structures and machines, and thus causes large amount of economic losses as well as safety hazards. Therefore, it is meaningful to evaluate the SCC susceptibility of martensitic stainless steel. The researches about SCC susceptibility and propagation behavior of metals have been widely carried out

and revealed meaningful results [8-10]. Several methods are adopted to study the SCC susceptibility of metals, such as slow strain rate technique [11-13], constant load SCC method [14], as well as C-rings test and so on [15].

05Cr17Ni4Cu4Nb is specified as a martensitic precipitation hardening stainless steel according to the standard of GB1220-2007, which is usually referred to as the 17-4PH. 1Cr12Ni3Mo2VN is kind of martensitic heat resistant steel and has good mechanical properties as well as corrosion resistance with the normal quenching and tempering heat treatment. These two martensitic stainless steels are widely used in some important industries such as energy and aviation. In many cases these two steels can be replaced by each other but with different cost. Their properties are strongly affected by carbon content. Therefore, The SCC susceptibility of 05Cr17Ni4Cu4Nb and 1Cr12Ni3Mo2VN were studied by electrochemical methods and complementary physical tests under constant load, in order to evaluate the stress corrosion resistance of these two martensitic stainless steels and offer a reference to engineering application.

2. EXPERIMENTAL

2.1 Materials

The specimens used in this study was commercial 05Cr17Ni4Cu4Nb and 1Cr12Ni3Mo2VN, their chemical compositions are listed in Table 1 and Table 2. It can be seen that 05Cr17Ni4Cu4Nb contains a higher content of Cr and Ni element and less Mn element compared to the 1Cr12Ni3Mo2VN. Besides, 05Cr17Ni4Cu4Nb includes a certain content of Cu and Nb element, while 1Cr12Ni3Mo2VN includes some Mo, V and N element. Another difference between these two steels is the C content which strongly affects the electrochemical corrosion properties of stainless steel.

Table 1. Chemical composition of 05Cr17Ni4Cu4Nb stainless steel (wt.%)

C	Cr	Ni	Mn	Nb	Cu
0.044	15.26	4.15	0.28	0.27	3.06

Table 2. Chemical composition of 1Cr12Ni3Mo2VN stainless steel (wt.%)

C	Cr	Ni	Mn	Mo	V	N
0.14	11.26	2.78	0.71	1.60	0.29	0.048

The testing samples of these two stainless steels were ground with a series of emery papers from 320 to 2000 grit, and subsequently polished using 250 nm diamond spay suspension, and then cleaned thoroughly with deionized water and alcohol in turn. The metallographic morphologies of the two stainless steels were observed by OLYMPUS (BX51M) optical microscope. And the relevant metallographic features of steels are shown in Fig.1. Both of these two stainless steels exhibit the typical

lath martensitic features as shown in Fig.1. The lath martensite in 1Cr12Ni3Mo2VN showed a smaller width than that in 05Cr17Ni4Cu4Nb. Lath martensite can effectively prevent the slipping of dislocations [16], and thus, the narrower martensite in 1Cr12Ni3Mo2VN performs less efficiency to prevent the dislocation slipping than the wider one in 05Cr17Ni4Cu4Nb.

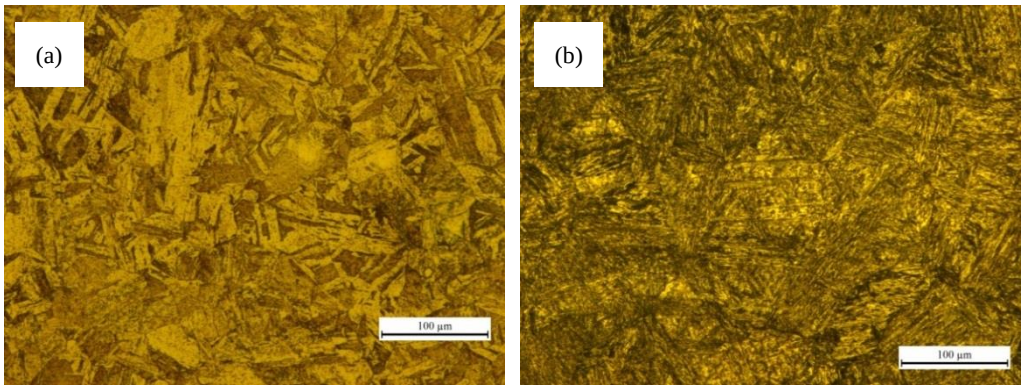

Figure 1. Metallographic features of two kinds of stainless steels, (a) 05Cr17Ni4Cu4Nb, (b) 1Cr12Ni3Mo2VN

2.2 Constant load stress corrosion test

The constant load SCC tests were performed in neutral 5 wt.% NaCl solution at the temperature of 298±1 K. The dimension of SCC testing samples is shown in Fig.2. The SCC tests were carried out at four stress levels (95%σ0.2, 90%σ0.2, 85%σ0.2, 80%σ0.2) using 3 valid parallel samples at each stress level. The yield strength of each sample was recorded after 120 h of SCC testing, in order to evaluate the strength loss and SCC resistance of such two kinds of martensitic stainless steels.

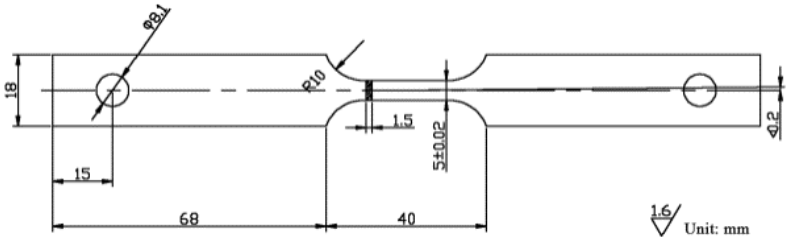

Figure 2. Dimension of the constant load SCC testing samples

2.3 Analysis of fracture morphology

After the constant load SCC tests, the corrosion products were removed and the fracture morphology of samples was observed by CamScan 3400 scanning electron microscope (SEM). Then the fracture morphologies of these stainless steels were compared.

2.4 Electrochemical measurements

Electrochemical measurements were carried out using a three-electrode system, where a saturated calomel electrode (SCE) acted as the reference electrode and a platinum foil acted as the auxiliary electrode. All of the potentials quoted in this study referred to the SCE. The electrodes were embedded in epoxy resin leaving a working area of 1.0 cm^2 to perform electrochemical tests. The working electrode preparation was carefully controlled to ensure that there was no gaps and bubble existing at the epoxy/steel interface. Prior to the electrochemical tests, the working surface of electrode was ground by 2000# emery paper and subsequently rinsed with deionized water and alcohol. Electrochemical measurements were carried out after 30 min immersion in order to obtain a steady state of working electrode. The experimental solution was neutral 5 wt.% NaCl, which was consistent to that used in constant load SCC test.

The potentiodynamic polarization tests were started at -250 mV relative to the open circuit potential (OCP), and the potential scanned to the positive direction with a scan rate of 0.5 mV/s until the anodic current density reached 10 $\mu A/cm^2$. The polarization curves of stainless steel were analyzed by Tafel extrapolation analysis. The electrochemical impedance spectroscopy (EIS) measurement of stainless steel electrode was carried out at the OCP using an AC stimulus signal of 10 mV with the frequency range from 10 mHz to 100 kHz.

3. RESULTS AND DISCUSSION

3.1 SCC susceptibility of steels

Table 3. Yield strength and strength loss of 05Cr17Ni4Cu4Nb samples after 120 h SCC tests under different stress levels

Stress Level ($\sigma_{0.2}$)	Yield Strength (σ_b/MPa)	Elongation (δ_5/%)	Strength loss ($\Delta\sigma_b$/%)
--	1433.41	6.60	--
95%	1389.64±26.61	6.30±0.12	3.05±0.36
90%	1398.10±23.38	5.48±0.08	2.46±0.29
85%	1425.31±19.76	5.10±0.08	0.57±0.15
80%	1430.36±16.52	4.95±0.05	0.21±0.07

Table 4. Yield strength and strength loss of 1Cr12Ni3Mo2VN samples after 120 h SCC tests under different stress levels

Stress Level ($\sigma_{0.2}$)	Yield Strength (σ_b/MPa)	Elongation (δ_5/%)	Strength loss ($\Delta\sigma_b$/%)
--	1209.77	7.78	--
95%	1164.32±27.61	7.20±0.13	3.76±0.43
90%	1172.39±27.95	7.05±0.11	3.09±0.35
85%	1192.59±23.93	7.03±0.08	1.42±0.22
80%	1203.84±20.37	6.98±0.08	0.49±0.11

The yield strength and the associated strength loss of those steel samples after 120 h SCC tests under different stress levels are listed in Tables 3 and 4 to evaluate the stress corrosion resistance of these two martensitic stainless steels. The data of specimens without SCC tests are also listed in Tables 3 and 4 to provide references.

The original yield strength of 05Cr17Ni4Cu4Nb (1433.41MPa) without SCC test is higher than that of 1Cr12Ni3Mo2VN (1209.77MPa); but the tensile elongation of steels shows a contrast pattern, i.e. 1Cr12Ni3Mo2VN shows a bigger tensile elongation. Table 3 and Table 4 show the similar regulations that both these two martensitic stainless steels show significant decrease in yield strength when they are suffering SCC. A higher stress level of SCC test usually results in a bigger strength loss of steels, and thus the strength loss percentage of steels decreases with the decreasing stress levels. A lower stress level during SCC test can delay the crack initiation time and reduce the cracking propagation rate in metal matrix in corrosive environment, therefore, the steels exhibit a smaller strength loss when suffering a lower stress level SCC [8-10].

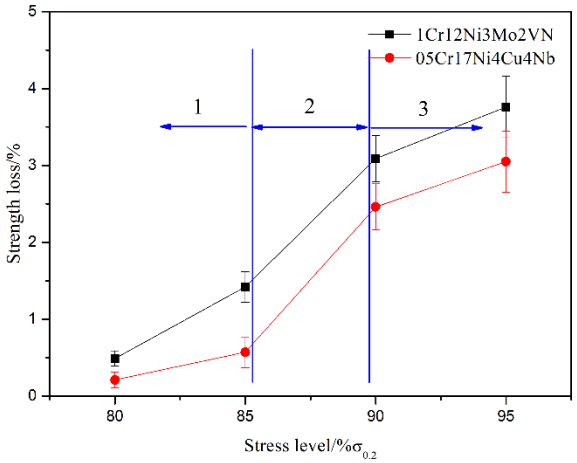

Figure 3. Strength loss percentage of two kinds of martensitic stainless steels after 120 h SCC tests with different stress levels

Fig.3 shows the strength loss of these two martensitic stainless steels after 120 h SCC tests with different stress levels. It clearly shows that the strength loss of steels does not exhibit a linear relationship with the SCC test stress levels. The curves in Fig. 3 can be divided into three regions. The ratio of strength loss to stress level in region 3 and region 1 is lower than that in region 2, indicating that the martensitic stainless steel shows a relatively higher SCC susceptibility at the 85-90%σ0.2 stress level. Even though, these two steels exhibit the similar change trend of strength loss vs. the stress level, the 05Cr17Ni4Cu4Nb exhibits a better SCC resistance compared to the 1Cr12Ni3Mo2VN due to the 05Cr17Ni4Cu4Nb showing a smaller strength loss at the same stress level. This may attribute to the low C element content and high Cr element content in 05Cr17Ni4Cu4Nb, which would improve the corrosion resistance of steels [9]. The detailed illustration about the corrosion resistance of steels was listed in section 3.3.

3.2 Fracture morphology of steels after SCC test

Fig.4 shows the original fracture appearance of 05Cr17Ni4Cu4Nb and 1Cr12Ni3Mo2VN after tensile test without SCC testing. Fig.5 shows the typical fracture feature of steels after 120 h SCC test in 5 wt.% NaCl solution under the stress level of 95%$\sigma_{0.2}$. As shown in Fig. 4, The fracture surfaces of the two stainless steel without SCC exhibit typical dimple feature, indicating that the fracture of martensitic stainless steel without SCC is typical ductile fracture. The number of dimples on fracture surface in 1Cr12Ni3Mo2VN is higher than that in 05Cr17Ni4Cu4Nb. While, the dimples in 05Cr17Ni4Cu4Nb shows a bigger size. The number of dimples on fracture surface in steels significantly decrease after 120 h SCC test as shown in Fig. 4 and Fig. 5, indicating that the SCC environment significantly deteriorates the ductility of these two martensitic stainless steels.

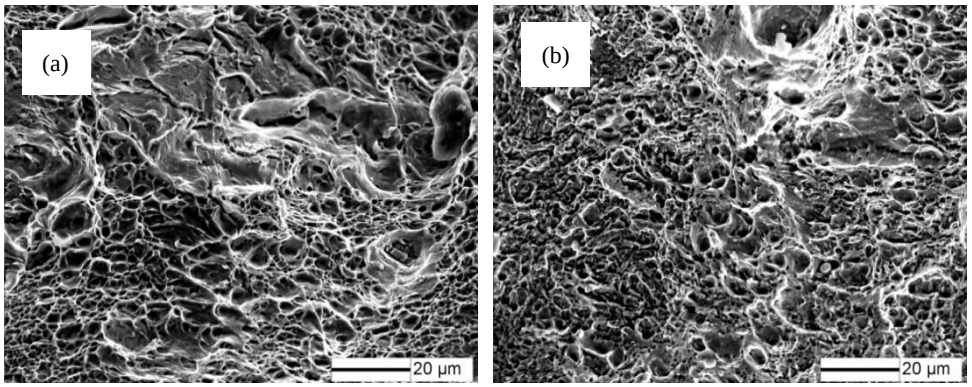

Figure 4. Fracture feature after tensile test of martensitic stainless steels without SCC testing, (a) 05Cr17Ni4Cu4Nb, (b) 1Cr12Ni3Mo2VN

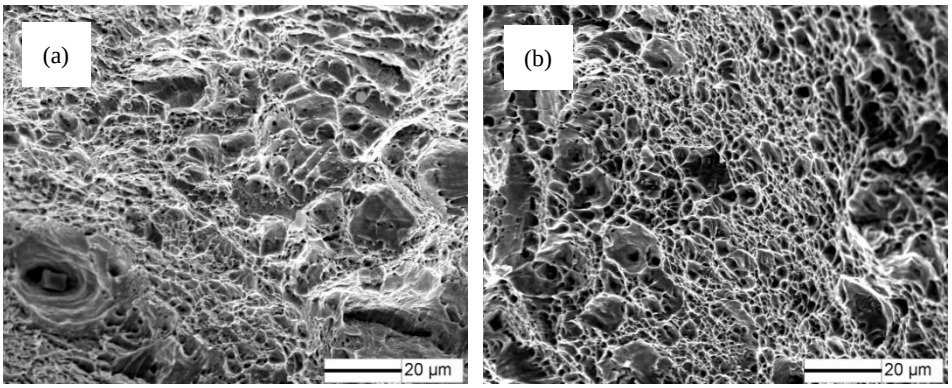

Figure 5. Fracture feature of martensitic stainless steels after 120 h SCC test at the stress level of 95%$\sigma_{0.2}$, (a) 05Cr17Ni4Cu4Nb, (b) 1Cr12Ni3Mo2VN

The alloy elements such as Cu and Nb help to strengthen the grain structure by precipitating at grain boundary during heat treatment [17]. The alloy elements of Cr, Ni can significantly improve the strength, hardness and wear resistance of the steel. For stainless steels in an aggressive atmosphere, the formation of a dense and good adhesive Cr_2O_3 film is able to limit the diffusion of elements between the steel and the outer solution environment, and thus prevent the further degradation of mechanical

properties of steels during corrosion. Fe containing oxides, such as (Fe, Ni) (Fe, Cr)$_2$O$_4$, are considered to be less effective to reduce the damage of metal matrix in corrosive environment, as they are less stable and easily broke away from the metal surface [18]. The Cr element is good to the corrosion resistance of steels when its content reaches at least 12 wt.%, but it reduces the plasticity and toughness of the steels meanwhile. In addition, the Mo element can play a favorable role in improving the toughness of steels. A more C element in metal matrix usually reduce the corrosion resistance of stainless steel, because it usually reacts with Cr element to form metal carbide and thus reduces the effective Cr content. Based on the above reasons, the yield strength and the SCC resistance of 05Cr17Ni4Cu4Nb are both higher than that of 1Cr12Ni3Mo2VN as shown in Tables 3 to 4 and Figs. 3 to 5.

3.3 Electrochemical measurement

The potentiodynamic polarization curves of martensitic stainless steels in 5 wt.% NaCl solution are shown in Fig. 6. The Tafel extrapolation was used to analyze the polarization curves to obtain detailed information about steels corrosion resistance. The relevant results are listed in Table 5.

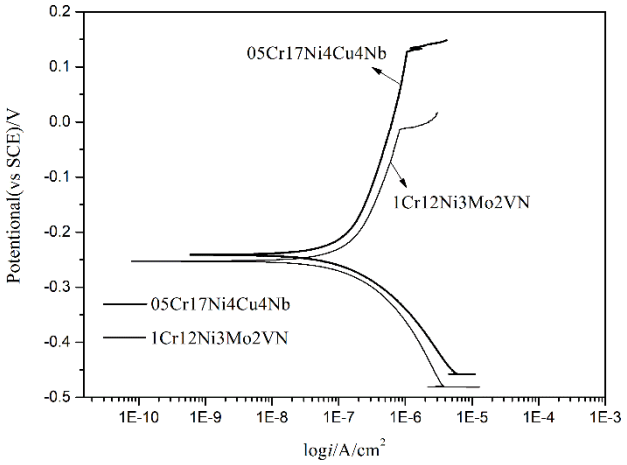

Figure 6. Potentiodynamic polarization curves of two kinds of martensitic stainless steels obtained in 5 wt.% NaCl solution

Table 5. Tafel extrapolation results of potentiodynamic polarization curves of the martensitic stainless steels

Materials	E_{corr}(mV)	i_{corr}(A/cm^2)	b_a(mV/decade)	-b_c(mV/decade)
05Cr17Ni4Cu4Nb	-246	1.468E-7	0.393	0.110
1Cr12Ni3Mo2VN	-255	1.307E-7	0.259	0.115

The E_{corr} values of such two kinds of stainless steels presented in Table 5 are very similar, though a relatively higher E_{corr} is observed on 05Cr17Ni4Cu4Nb. This may indicate that a more stable passive film is formed on the 05Cr17Ni4Cu4Nb surface. But the increment of E_{corr} value is so small that should be taken carefully as it could also be attributed to very small surface differences after the electrode preparation [19]. In addition, a passivation-like behavior in a wide range of anodic potentials is observed

in the curves. The passive range of 05Cr17Ni4Cu4Nb is from -0.15 V to 0.12 V, while the passive range of 1Cr12Ni3Mo2VN is from -0.15 to -0.02V. Hence the 05Cr17Ni4Cu4Nb has a wider passive potential range than the 1Cr12Ni3Mo2VN. Besides, the passive current of 05Cr17Ni4Cu4Nb also shows a smaller value. Based on the data shown in Table 5, it can be concluded that the corrosion resistance and the passivation property of 05Cr17Ni4Cu4Nb are better than that of 1Cr12Ni3Mo2VN.

Fig. 7 shows the Nyquist plots of EIS measurement to 05Cr17Ni4Cu4Nb and 1Cr12Ni3Mo2VN in 5 wt.% NaCl solution. The relevant Bode plots are shown in Fig. 8. In these plots *f* is the frequency and |Z| is the impedance modulus. The impedance modulus of 05Cr17Ni4Cu4Nb is higher than that of 1Cr12Ni3Mo2VN in medium and high frequency ranges. These comparative measurements show that both martensitic stainless steels exhibit a similar corrosion behavior in the same aggressive environment. In the medium frequency ranges, the impedance modulus in bode plots defined a straight line with a zero slope and the phase angle remained in zero degrees which indicates a resistive-like behavior rather than a relaxation process occurring on electrode surface [19]. The Nyquist and Bode plots showed two capacitive-like behaviors at the low and high frequencies which was characterized by the slanted impedance modulus and high phase angle.

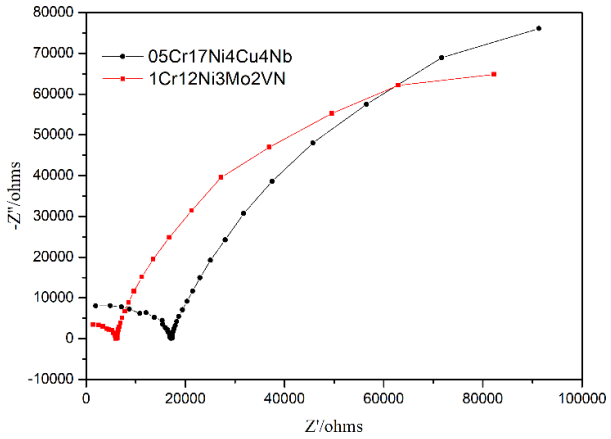

Figure 7. Nyquist plots of EIS measurements to 05Cr17Ni4Cu4Nb and 1Cr12Ni3Mo2VN in 5 wt.% NaCl solution

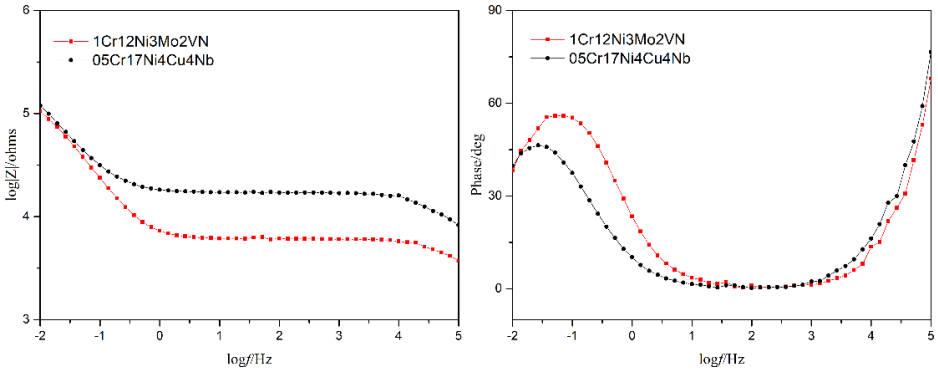

Figure 8. Bode plots of EIS measurements to 05Cr17Ni4Cu4Nb and 1Cr12Ni3Mo2VN in 5 wt.% NaCl solution

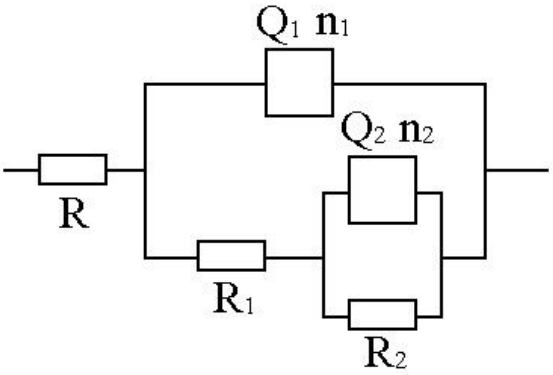

Figure 9. Equivalent circuit used to fit the EIS measurements plots

In order to obtain the quantitative information of EIS measurements, the impedance data was fitted using the electrical equivalent circuit (EEC) as shown in Fig. 9. Obviously, the time constant in the high frequency range was attributed to the passive film (R_1, n_1 and Q_1), and the another one in the low frequency range was attributed to the charge transfer reaction (R_2, n_2 and Q_2). The experimental diagrams are well fitted with the EEC, and the values of the fitted results are reported in Table 6.

Table 6. ECC Fitted results of EIS measurements for two kinds of martensitic stainless steels in 5 wt.% NaCl solution

Materials	R	Q_1	n_1	R_1	Q_2	n_2	R_2
05Cr17Ni4Cu4Nb	0.188	9.067E-10	0.892	1.705E4	6.779E-5	0.804	2.253E5
1Cr12Ni3Mo2VN	0.126	9.514E-10	0.945	6.046E3	6.935E-5	0.854	1.628E5

The Q_1 is an indicative parameter of the oxide film thickness [20]. As it can be seen from Table 6, 05Cr17Ni4Cu4Nb has a lower Q_1 value and a higher R_1 value than 1Cr12Ni3Mo2VN. This indicates that the passive film formed on 05Cr17Ni4Cu4Nb surface has a better corrosion resistance than that formed on 1Cr12Ni3Mo2VN. The adsorption of Cl^- on the film surface can accelerate the local dissolution of the passive film by chloride-catalyzed mechanism, which can result in the increasing of cation vacancy in the passive film [21]. According to the electrochemical results, it is more difficult for Cl^- ion to penetrate into the passive films formed on 05Cr17Ni4Cu4Nb during SCC test. And thus, the 05Cr17Ni4Cu4Nb has a better corrosion resistance and a smaller SCC susceptibility compared to 1Cr12Ni3Mo2VN.

4. CONCLUSIONS

(1) The strength loss percentage of 05Cr17Ni4Cu4Nb at the stress levels of 95%σ0.2, 90%σ0.2, 85%σ0.2 and 80%σ0.2 is 3.05%, 2.46%, 0.57% and 0.21%, respectively; and the corresponding strength loss of 1Cr12Ni3Mo2VN at such stress levels is 3.76%, 3.09%, 1.42% and 0.49%, respectively. The strength loss percentage of 05Cr17Ni4Cu4Nb is lower than that of the 1Cr12Ni3Mo2VN, and thus the 05Cr17Ni4Cu4Nb has a better SCC resistance.

(2) The fracture features for both steels are typical dimples, and the 1Cr12Ni3Mo2VN has more and smaller dimples than the 05Cr17Ni4Cu4Nb. In addition, the number of dimples on samples suffered SCC is less than that on the original one.

(3) The passive potential range of 05Cr17Ni4Cu4Nb (from -0.15 to 0.12V) is wider than that of the 1Cr12Ni3Mo2VN (from -0.15 to -0.02V). Besides, a better passive film is formed on the surface of 05Cr17Ni4Cu4Nb, which leads to a better corrosion and SCC resistance to the steel.

ACKNOWLEDGEMENTS
This research is sponsored by the Youth Fund of the Hebei Natural Science Fund project under Grant No. E2019409052, and the Education Department Science Research project of Hebei under Grant No. QN2019104.

References

1. W. Tian, S. Li, N.Du, S. Chen, and Q. Wu, *Corros. Sci.*, 93 (2015) 242.
2. W. Tian, N.Du, S. Li, S. Chen, and Q. Wu, *Corros. Sci.*, 85 (2014) 372.
3. W.M. Tian, Y.J. Ai, S.M. Li, N. Du, and C. Ye, *Acta Metall. Sin. (Engl. Lett.)*, 28 (2015) 430.
4. I. Bösing, I. Bobrov, J. Epp, M. Baune, and J. Thöming, *Int. J. Electrochem. Sci.*, 15 (2020) 319
5. M. Zhu, Y. Yuan, Q. Zhang, S. Yin, and S. Guo, *Int. J. Electrochem. Sci.*, 14 (2019) 1876.
6. Q. Li, H. Meng, Randou, X. Gong, B. Long, and R. Ni, *Int. J. Electrochem. Sci.*, 15 (2020) 109.
7. S. Chen, B. Zhu, and X. Liang, *Int. J. Electrochem. Sci.*, 15 (2020) 1.
8. P. Liang, Y. Guo, H. Qin, Y. Shi, F. Li, L. Jin, and Z. Fang, *Int. J. Electrochem. Sci.*, 14 (2019) 6247
9. M. W, Z. Zhao, X. Wang, J.C. Huang, and X. Liu, *Int. J. Electrochem. Sci.*, 15 (2020) 208.
10. S. Luo1, M. Liu, N. Wen, Y. Shen, Y. Liu, and X. lin, *Int. J. Electrochem. Sci.*, 14 (2019) 2589.
11. L.F. Wu, S.M. Li , J.H. Liu, and M. Yu, *J. Cent. South. Univ.*, 19 (2012) 2726.
12. S.Y. Chen, K.H. Chen, and G.S. Peng, *T. Nonferr. Metal. Soc.*, 22 (2012) 47.
13. F. Zanotto, V. Grassi, A. balbo, C. Monticelli, and F. Zucchi, *Corros. Sci.*, 80 (2014) 205.
14. A. Venugopal, R. Panda, S. Manwatkar, K. Sreekumar, L.R. Krishna, and G. Sundararajan, *T. Nonferr. Metal. Soc.*, 22 (2012) 700.
15. J.S. Baek, J.G. Kim, D.H. Hur, and J.S. Kim, *Corros. Sci.*, 45 (2003) 983.
16. H. Kitahara, R. Ueji, and N. Tsuji, *Acta Mater.*, 54 (2006) 1279.
17. H. Guo, J. Cheng, S. Yang, and X. He, *J. Alloy. Compd.*,577 (2013) 619.
18. A. Malfliet, M. Campforts, and B. Blanpain, *Corros. Sci.*, 57 (2012) 1.
19. S. Fajardo, D.M. Bastidas, M. Criado, and J.M. Bastidas, *Electrochim. Acta*, 129 (2014) 160.
20. S. Marcelin, N. Pebere, S. Regnier, *Electrochim. Acta*, 87 (2013) 32.
21. S. Ahn, H. Kwon, D. D. Macdonald. *J. Electrochem. Soc.*, 152 (2005) B482.